Sigma Journal of Engineering and Natural Sciences
Web page info: https://sigma.yildiz.edu.tr
DOI: 10.14744/sigma.2025.00042

Research Article

Prediction of the compressive strength in high-strength concrete cores through the destructive method

Salem MERABTI[1,*], Salah BEZARI[2], Abdellah BOUDINA[3]

[1]*Acoustics and Civil Engineering Laboratory, Faculty of Sciences and Technology, Khemis-Miliana University, Road of Theniet el Had, Khemis Miliana 44225, Algeria*
[2]*Unité de Recherche Appliquée en Energies Renouvelables URAER, Centre de Développement des Energies Renouvelables CDER, Ghardaïa 47133, Algeria*
[3]*Laboratory of Fluid Industrials, Measures & Application (FIMA), Faculty of Science and Technology, University Djilali Bounaama of Khemis-Miliana, 44225, Algeria*

ARTICLE INFO

Article history
Received: 15 March 2024
Revised: 13 May 2024
Accepted: 03 August 2024

Keywords:
Cast Specimen; Compressive Strength; Core Drilling; Cure Environment; Destructive Test; High-Strength Concrete

ABSTRACT

Destructive testing (DT) was conducted on high-strength concrete to explore the influence of various factors on its compressive strength. Specifically, three types of core samples were extracted from blocks with length-to-diameter (L/D) ratios of 1 and 2. Additionally, three other types of cast specimens with an L/D ratio of 2 were produced from the same composition. The results of the compressive tests were individually and collectively compared with standard cylindrical specimens. Correlations were established with standard cylindrical specimens to predict the compressive strength of different sizes of cores and cast specimens. Various statistical indicators, including root mean square error (RMSE) and standard deviation (SD), were evaluated to ensure the accuracy of the correlation predictions. The analysis of the results indicates that the L/D ratio, curing method, and specimen size impact the compressive strength of high-strength concrete. However, specimen size was found to have the most significant influence on the specimens' response. The best estimation of the compressive strength of cores compared to standard cylinders was obtained using exponential models. These models provided accurate estimates in terms of statistical indicators. The lowest coefficients of variance (CV) and average relative error (ARE), which ensure high precision, were recorded for cores with an L/D ratio of 2. Depending on the L/D ratio, the diameter of the cores, and the storage environment of the standard cylinders, the conversion factors for high-strength concrete cores varied between 0.543 and 0.972. Further research should focus on refining these conversion factors and exploring the effects of other variables on high-strength concrete's compressive strength.

Cite this article as: Merabti S, Bezari S, Boudina A. Prediction of the compressive strength in high-strength concrete cores through the destructive method. Sigma J Eng Nat Sci 2025;43(2):541–554.

***Corresponding author.**
*E-mail address: s.merabti@univ-dbkm.dz

This paper was recommended for publication in revised form by Editor-in-Chief Ahmet Selim Dalkilic

INTRODUCTION

Concrete is widely used worldwide for the construction of structures of various sizes, whether they are large, medium, or small [1-4]. According to Monteiro et al. [5] 30 billion tons of concrete are produced globally each year. Generally, the nominal compressive strength is the most important property of concrete, and it is determined at 28 days of age [6-8]. This strength is tested on standard-shaped specimens, such as cylinders with a diameter of 150 mm and a length of 300 mm or cubes with sides of 150 mm [9, 10]. To this end, several studies have been conducted to convert the strength of cylinders to the strength of cubes, and a factor of 1.2 has been proposed for ordinary concrete [11, 12]. However, this factor decreases with the increase in concrete strength. The IS 516 (Part 4): 2018 standard recommends that the equivalent strength of a cylinder with a length-to-diameter ratio of 2 should be corrected by a correction factor of 1.25 compared to a cube [13]. However, when it comes to in-situ testing (destructive testing) to verify the quality of concrete, non-standard-sized specimens referred to as cores are commonly used. Cores are smaller in size compared to standard cylindrical specimens, which are referred to as the scale effect [14]. Compared to other non-destructive tests, these destructive tests provide more accurate compressive strengths [15, 16]. It would be prudent, therefore, to evaluate compressive strength using concrete cores.

The compressive strength of cores obtained through coring (destructive testing) of both old and new structures can be influenced by the size of the specimens [17]. Numerous experimental studies in the literature examine the impact of specimen size and shape [18-21]. For instance, authors [22, 23] established a linear correlation between the compressive strengths of cubes and microcores. Chockalingam et al. [24] simultaneously investigated the effects of specimen shape, size, and aggregate size, noting that as aggregate size and specimen length increase, compressive strength, splitting tensile strength, and flexural strength decrease. A recent study examined the effects of sample size, aggregate size, and compressive strengths between 25 MPa and 30 MPa [13]. Zhu et al. [25] established the role of aggregate and sample size on the overall fragility of the structure.

Other researchers have explored the influence of the maximum aggregate size on the strength of microcores [26, 27]. The smallest dimensions of microcores tested were 28 mm, as studied by Indelicato and Kilinc et al. [9, 28]. Regarding regulations, the American standard ASTM C42 for obtaining drilled cores requires a dimension of 95 mm [29]. In contrast, the new European standard EN 13791:2019 [30] requires a dimension of 100 mm and recommends that core size be at least three times the maximum aggregate size used in concrete production. It is worth noting that ISO/DIS 7032 [30,31], DIN 1048 Teil 2 [32], and the guidelines of ACI Committee 301 [33] permit the use of cores smaller than 50 mm in specific situations.

Various studies have suggested increasing the number of smaller-sized cores [9, 34]. According to the study conducted by Vasanelli et al. [35], the limited number of extracted cores does not provide a faithful representation of the concrete strength in the examined structure. The accurate conversion of core results relative to standard specimens is directly dependent on the number of cores extracted. Moreover, uncontrolled factors constitute sufficient reasons to increase the number of cores [36]. Following the research by Boussahoua et al. [37], the minimum number of cores that ensure a proper evaluation of concrete strength is seven to nine cores. According to the authors, statistical origin error is strongly influenced by the number of cores. However, Alwash et al. [38] note that precision adds little value beyond seven to eight cores, and other authors [39, 40] have concluded that compression strength stabilization occurs from nine cores onward. Contrary to specific standards such as EN 13791 [39], ACI 228 1R [41], and NA17004 [42], which recommend reducing the number of cores to avoid compromising the strength of structures.

The mechanical properties of cores are influenced by several factors. For instance, researchers [10, 43] have highlighted various elements affecting core performance, including moisture, the length-to-diameter ratio (L/D), drilling direction, and the type of coring equipment used. However, there are still many factors in this domain that remain to be explored. The standards commonly applied for coring in existing structures include the American Concrete Institute (ACI) standards [41, 44, 45] and European standards [30, 46]. The mentioned studies predominantly focus on ordinary concrete containing coarse aggregates. Nevertheless, there is a scarcity of research focused on concrete designed for thin elements, such as slabs and walls [47-49]. However, literature reveals that several studies have been conducted using non-destructive tests to assess the quality of concrete. For instance, Ju et al. [50] estimated the compressive strength of high-strength concrete (HSC) from nuclear power plants using non-destructive tests on concrete specimens up to 100 MPa. The authors compared results from 30 mm, 50 mm, and 100 mm cores with those obtained from non-destructive tests. Similarly, Wankhade and Landage [51] conducted a study on a water reservoir and emphasized the importance of these non-destructive tests in identifying and detecting internal defects and cracks in concrete. However, the combined use of non-destructive tests to assess concrete strength in structures was examined by Jain et al. [52]. The validation of non-destructive tests is thus performed through destructive tests, granting them crucial importance. Ivanchev [53], along with Shrestha and Giri [54], introduced these two methods for the evaluation of compressive strength.

This study aims to assess the ability to predict the compressive strength of high-strength concrete based on compression strength tests of cores and cast specimens. The correlation of compressive strength is examined across various core sizes and standard cylindrical specimens,

Table 1. Chemical composition of cement (%)

SiO_2	AL_2O_3	Fe_2O_3	CaO	MgO	K_2O	Na_2O	SO_3	CaO free	Insoluble	Loss on ignition
20.19	5.23	3.34	56.9	2.01	0.61	0.15	2.31	1.01	2.41	5.84

considering the effects of the curing environment. With the insights drawn from the results, it will become feasible to estimate the in-situ compressive strength of concrete and suggest the minimum number of cores needed for accurate predictions according to the established conversion model.

EXPERIMENTAL DESIGN

Materials Used

High-strength concrete was prepared using standard Portland cement of type CEM II/A 42.5. At the age of 28 days, this binder exhibits a compressive strength of 45.78 MPa and a flexural strength of 8.47 MPa. The chemical properties of the binder are detailed in Table 1.

Table 2 presents the detailed properties of the 0/3.15 sand and 3/8 gravel used, while Figure 1 illustrates their respective particle size distribution.

Concrete Preparation

A compressive strength of concrete exceeding 45 MPa has been developed, considered as high strength according to ACI 213R and DTR BC248 [55, 56]. This compressive strength was measured following ASTM C469 and ASTM

Table 2. Physical characteristics of fine and coarse aggregates

Characteristics	Sand	Gravel
Granular class	0/3.15	3/8
Apparent density (Kg/m^3)	1480	1500
Absolute density (Kg/m^3)	2520	2500
Thinness module	2.11	-
Sand equivalent (%)	82	-
Cleanliness of gravel (%)	-	1.4

Table 3. Mixture proportions

Concrete	Sand (Kg/m^3)	Gravel (Kg/m^3)			Cement (Kg/m^3)	Water (l/m^3)
	0/3	3/8	8/15	15/25		
C45/55	533	1073	-	-	493	211

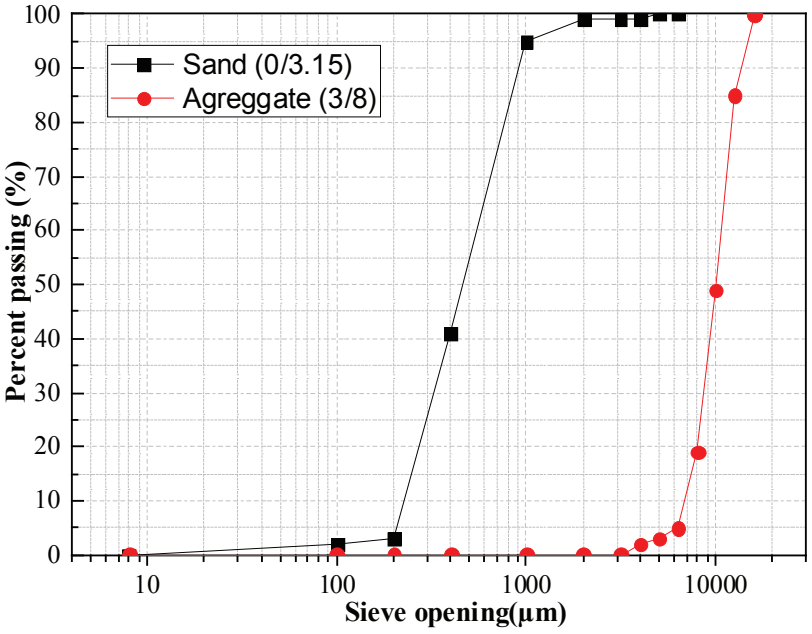

Figure 1. Particle size distribution of the sand and aggregate.

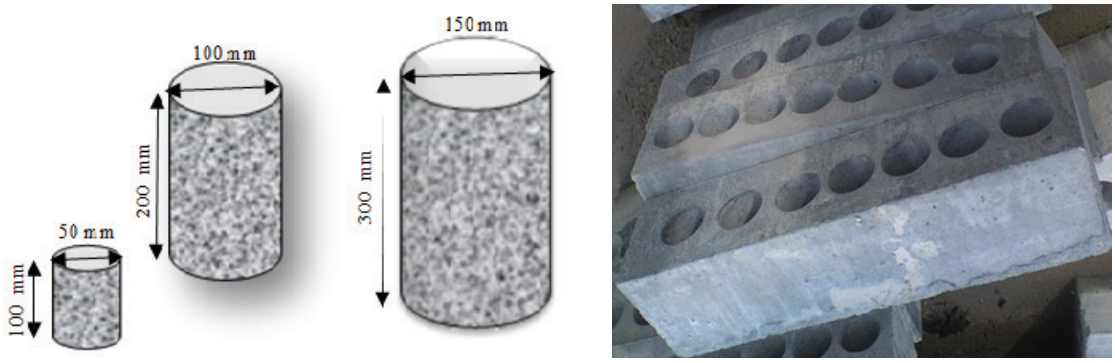

a) b)

Figure 2. Tested concretes: (a) Cast specimen, (b) Concrete blocks for core drilling.

C39 on cylinders with a diameter of 150 mm and a height of 300 mm [57, 58]. The materials used in the concrete mix include sand, aggregates, Portland cement, and tap water, as presented in Table 3. The Dreux-Gorisse method was employed as the concrete formulation method.

Specimens Produced

The experimental program is conducted in two series of tests, involving cast specimens as well as cores extracted from the same concrete. The first series, comprising 36 cast specimens with diameters of 50 mm, 100 mm, and 150 mm and a length-to-diameter ratio equal to 2 (L/D=2), was subjected to two environmental conditions: exposed to air (natural conditions) and submerged in water at 20 °C (Fig. 2a). The second series involves extracting 27 cores from blocks with diameters of 50 mm, 75 mm, and 100 mm, nine cores for each type (see Fig. 2b). It is noteworthy that these blocks were exposed to open air. Core drilling was performed following ASTM C42 [29], and compression tests were conducted within 7 days of coring. Before testing, the cores were prepared following the guidelines of standard NA 5071 and DIN EN 12.504-1 [59, 60]. In this research, two length-to-diameter ratios equal to 1 and 2 were used for the cores, with their extraction performed in the direction of concrete casting.

Table 4 summarizes the densities of the cast specimens as well as the cores extracted from the concrete blocks. These values represent the averages of nine specimens obtained at the age of 28 days, all made with the same concrete mix. The standard deviation and coefficient of variation values are provided for each studied specimen.

To better present the experimental results, various forms of conversion models were tested, namely linear regression (1), power function (2), exponential function (3), logarithmic function (4), and polynomial function (5). These forms are commonly employed in the literature to assess

Table 4. Mean densities of cast specimens and cores

		Density of cast specimen			
Cure	**L/D**	**Dimensions (mm)**	**Density (t/m³)**	**SD**	**CV (%)**
		50x100	2.398	0.069	2.877
Water	2	100x200	2.401	0.020	0.833
		150x300	2.394	0.007	0.292
		50x100	2.347	0.050	2.130
Air	2	100x200	2.389	0.016	0.670
		150x300	2.362	0.018	0.762
		Density of crushing cores			
		50x50	2.255	0.020	0.882
Air	1	75x75	2.317	0.022	0.955
		100x100	2.352	0.038	1.613
		50x100	2.273	0.014	0.614
Air	2	75x150	2.345	0.070	2.965
		100x200	2.379	0.041	1.738

the compressive strength of concrete in existing structures [15, 61, 62].

$$f_1 = \text{a D} + b \quad (1)$$

$$\text{f}_2 = \text{a D}^{\text{b}} + \text{c} \quad (2)$$

$$\text{f}_3 = \text{a exp}^{\text{bD}} + \text{c} \quad (3)$$

$$\text{f}_4 = \text{a lnD} + \text{b} \quad (4)$$

$$\text{f}_5 = \text{a D}^2 + \text{bD} + \text{C} \quad (5)$$

With:

$f = \bar{f}_{c(d)}/\bar{f}_{c(150)}$ or $f = \bar{f}_{p(d)}/\bar{f}_{c(150)}$

$\bar{f}_{c(d)}$: Mean compressive strength of cores in MPa,

$\bar{f}_{c(150)}$: Mean compressive strength of standard cast specimens preserved in water or air, depending on the combination

D: Core diameter in mm.

The parameters a, b, and c were accurately determined from the experimental data using the least squares method. To assess the quality of the conversion model, statistical indices such as standard deviation, coefficient of variation, and coefficient of determination are utilized. Additionally, the standard deviation (SD) of the model concerning the mean compressive strength and the root mean square error (RMSE) of prediction have been used to assess the disparity between the compressive strength predicted by the model and the experimental strength. These indices have been calculated according to equations (6) and (7).

$$RMSE = \sqrt{\frac{1}{N}\sum_{i=1}^{N}\left(f_{ci}^{exp} - f_{ci}^{cal}\right)^2} \quad (6)$$

$$SD = \sqrt{\frac{1}{N}\sum_{i=1}^{N}\left(f_{ci}^{cal} - \overline{f_{mean}^{cal}}\right)^2} \quad (7)$$

Where $\text{f}_{\text{ci}}^{\text{exp}}$ is the experimentally obtained compressive strength, $\text{f}_{\text{ci}}^{\text{cal}}$ is the compressive strength calculated by the proposed model, and $\overline{\text{f}_{\text{mean}}^{\text{cal}}}$ is the mean compressive strength of the model.

EXPERIMENTAL RESULTS

Case of Cores with L/D = 1

Individual simulation of the compressive strength of various cores compared to that of standard specimens, whether stored in water or air, was conducted. In total, 81 simulations were performed. To establish an appropriate relationship between the diameter (D) of the cores and the compressive strength ratios $f_{c(d)}/f_{c(150}$), correlations were conducted based on (D) and the curing method. Five different mathematical equations were tested, and equation selection was based on an analysis of four statistical indicators, including the coefficients of determination, correlation coefficient, coefficient of variation, and mean relative error. From the results obtained in Table 5, it is evident that the coefficient of variation (CV) and average relative error (ARE) are low for the exponential function in both curing conditions. As depicted in Figure 3, equations 8 and 9 were chosen as the ideal representations of the correlation between the diameter (D) of the cores and the ratios $f_{\text{p(d)}}/f_{\text{c(150}}$), with the first equation applying to wet curing and the second to air curing. This equation format was also selected for non-destructive tests [63- 65].

$$f_3 = 0.3138\text{exp}^{0.0106D} - 0.080 \quad (8)$$

$$\text{f}_3 = 0.3398\text{exp}^{0.0106\text{D}} - 0.087 \quad (9)$$

Table 5. Regression formulas used and associated statistical indices (L/D=1)

	$\bar{f}_{\text{c(150)}}$ **in water**			
Function form	R^2	R	CV (%)	ARE (%)
f_1 = 0.0079 D + 0.022	0.622	0.789	21.221	19.316
f_2 = 0.0313 D0.7245- 0.0995	0.606	0.779	22.644	19.172
f_3 = 0.3138e0.0106D - 0.080	0.663	0.815	17.466	14.919
f_4 = 0.5398 ln(D) - 1.5884	0.561	0.749	26.382	23.974
f_5 = 0.0003D2 - 0.0304D + 1.012	0.741	0.861	27.558	21.044
	$\bar{f}_{\text{c(150)}}$ **in air**			
f_1 = 0.0086 D + 0.020	0.630	0.793	21.268	19.442
f_2 = 0.0339 $D^{0.7245}$ - 0.109	0.613	0.783	22.798	19.367
f_3 = 0.3398$e^{0.0106D}$ - 0.087	0.672	0.820	17.533	15.005
f_4 = 0. 5844 ln(D) - 1.858	0.568	0.754	24.025	24.025
f_5 = 0.0003D^2 - 0.0329D + 1.342	0.734	0.857	32.347	23.225

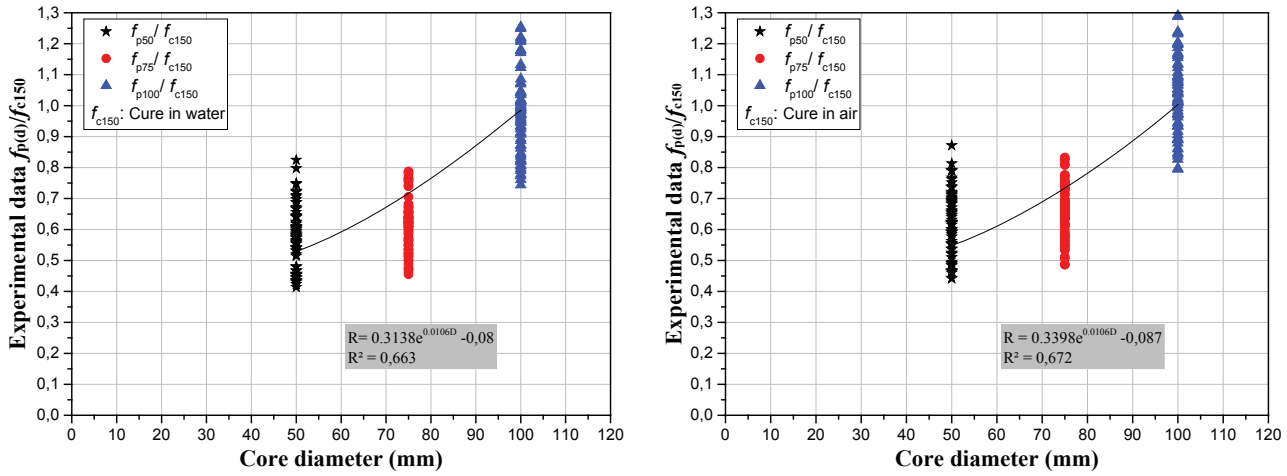

a) b)

Figure 3. Size effect for cores L/D=1. (a): Cure in water, (b): cure in air.

Figure 3 illustrates the ratios of 50 mm, 75 mm, and 100 mm cores to standard specimens $f_{p(d)}/f_{c(150)}$, where the L/D ratio is 1. The presented results below are individual ratios from 81 simulations. The colors black, red, and blue correspond to 50 mm, 75 mm, and 100 mm cores, respectively. Conditional coring was performed, and the cores were meticulously prepared following the previously mentioned standards.

The individual simulation results show that 60.49% of the $f_{p(100)}/f_{c(150)}$ ratios are below 1, with an average of 0.972 (Fig 3a). In contrast, the $f_{p(75)}/f_{c(150)}$ and $f_{p(50)}/f_{c(150)}$ ratios are all below 1, with averages of 0.615 and 0.576, respectively. Thus, it can be observed that the compression results of the 100 mm cores are close to 1, while the other two cores require correction factors, despite their low slenderness (L/D=1). Equation (3) was selected as the most appropriate relationship, and model analysis provided us with a coefficient of determination R^2 equal to 0.663.

The ratios $f_{p(d)}/f_{c(150)}$ obtained from the experimentation show an increase when $f_{c(150)}$ is cured in the air. Indeed, the average of the $f_{p(100)}/f_{c(150)}$ ratios is 1.05, demonstrating a slight superiority of the $f_{p(100)}$ cores in this specific context. However, the averages of $f_{p(75)}/f_{c(150)}$ and $f_{p(50)}/f_{c(150)}$ ratios are 0.665 and 0.624, respectively. An increase in these ratios is observed compared to curing in water. In the case of air curing, the suggested exponential model (Fig. 3b) has a coefficient of determination (R^2) equal to 0.672.

Below presents the variation of the Root Mean Square Error (RMSE) with the number of cores for the coring technique, as well as the standard deviation (SD) of the conversion model calculated according to equation 6 (Fig. 4). These two statistical parameters are related to the curing environment. A decrease in prediction error (RMSE) is observed with an increase in the number of cores in both curing environments, but the stability of the RMSE error seems to manifest only from 8 to 9 cores for the 75 mm and 100 mm cores in the case of wet curing (Fig. 4a). On the other hand, no stability in the RMSE error was observed for the 75 mm and 100 mm cores in air curing. This is likely due to the influence of the L/D ratio of 1. However, stability in the 75 mm cores was observed in both curing conditions, from 5 cores, corresponding to strength of about 2 MPa.

The standard deviation (SD) of our conversion model, measured during the determination of $f_{c(150)}$ in water, stabilizes from 6 cores onward (Fig. 4b). There is a slight variation in compression between 6 and 9 cores of different sizes. The 100 mm core exhibits the maximum standard deviation of the model, reaching 3 MPa. Stabilization in the case of air curing is observed between 5 and 7 cores, and then increases slightly for compressive strengths equivalent to those obtained with water curing (Fig. 4d). This is due to the curing conditions of high-strength concrete (in the open air), meaning the increase in uncontrolled parameters such as humidity and temperature, reducing the quality of the conversion model. However, increasing the number of cores will stabilize the standard deviation (SD) and the root mean square error (RMSE) of the exponential model.

Table 6 presents the ratios between the cores and cast specimens of the same dimensions with the L/D ratio for cores equal to 1. The mean values, standard deviation (SD), and coefficient of variation of the compressive strengths of the cores were calculated based on 81 simulations.

Overall, a prevalence of core strengths over cast specimens was observed. Analyzing the statistical indicators, it is noted that the $f_{p(50)}/f_{c(150)}$ ratio of specimens cured in air exhibits a higher standard deviation and coefficient of variation.

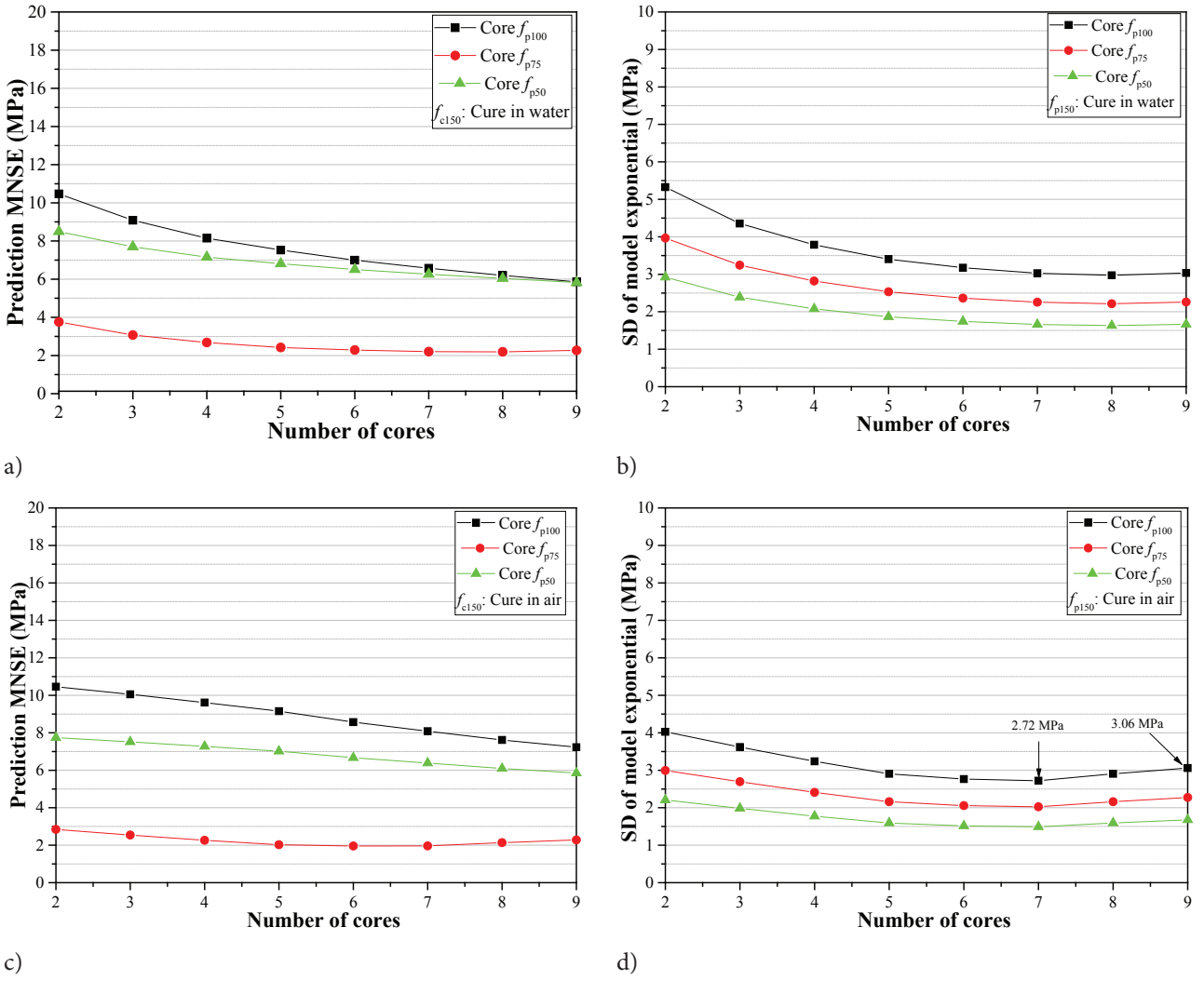

Figure 4. RMSE and SD of the prediction model as a function of the number of cores: Case of L/D=1. (a) and (b): Cure in water, (c) and (d): cure in air.

Table 6. Comparison of different cores with cast specimens

	($f_{c(d)}$) cure in water		($f_{c(d)}$) cure in Air	
	f_{p100}/f_{c100}	f_{p50}/f_{c50}	f_{p100}/f_{c100}	f_{p50}/f_{c50}
Arithmetic mean	1.390	1.120	1.173	1.156
Standard Deviation	0.234	0.102	0.153	0.253
Coef of variation (%)	16.835	9.091	13.043	21.886

Case of Cores with L/D = 2

The five equation forms were also tested in the case of D/L=2 and both curing conditions (see Table 7). Among these equations, the exponential function also stands out with lower coefficients of variation (CV) and average relative errors (ARE). Thus, equations 10 and 11 were selected as optimal expressions for the compressive strength curve of high-strength concrete (Fig. 5). For this equation form, the coefficients of determination (R^2) and correlation (R) are higher in the case of air curing. However, these coefficients, in the case of water curing, remain lower than those of the polynomial equation, but the latter exhibits higher coefficients of variation (CV) and average relative errors (ARE). This allows us to retain the logarithmic fitting curves for the experimental results, with a coefficient of variation (CV) below 17% valid for both curing

Table 7. Regression formulas used and associated statistical indices (L/D=2)

$\overline{f}_{c(150)}$ in water				
Function form	**R^2**	**R**	**CV (%)**	**ARE (%)**
$f_1 = 0.008D - 0.053$	0.755	0.869	20.437	19.310
$f_2 = 0.018D^{0.83} - 0.089$	0.745	0.863	21.558	18.470
$f_3 = 0.2594e^{0.012D} - 0.069$	0.802	0.895	15.780	13.559
$f_4 = 0.569\ln(D) - 1.887$	0.692	0.832	26.200	24.703
$f_5 = 0.0002D^2 - 0.0257D + 1.29$	0.848	0.921	31.054	24.371
$\overline{f}_{c(150)}$ in air				
$f_1 = 0.009D - 0.057$	0.764	0.874	20.189	19.016
$f_2 = 0.0199D^{0.83} - 0.098$	0.754	0.868	21.280	18.199
$f_3 = 0.2809e^{0.012D} - 0.073$	0.807	0.898	15.640	13.418
$f_4 = 0.6162\ln(D) - 2.042$	0.700	0.837	25.964	24.401
$f_5 = 0.0002D^2 - 0.0278D + 1.437$	0.646	0.804	37.718	26.948

environments of $f_{c(150)}$. However, in the case of D/L=1, it is observed that the coefficient is above 17% in both curing environments.

$$f_3 = 0.2594\exp^{0.012D} - 0.069 \quad (10)$$

$$f_3 = 0.2809\exp^{0.012D} - 0.073 \quad (11)$$

An exponential trend was also observed. The results presented in Figure 5 show the ratios $f_{c(d)}/f_{c(150)}$ as a function of core diameters (D), this time with an L/D ratio of 2. An increase in the ratios $f_{p(d)}/f_{c(150)}$ is noted with the increase in core diameter. The relationships obtained exhibit higher R^2 coefficients compared to L/D=1. The experimental results yield ratios below 1. The average differences in compressive strengths between the conversion model and experimental results in a wet environment ($f_{c(150)}$) are 19.44%, 0.43%, and 13.25% for the 50 mm, 75 mm, and 100 mm cores, respectively. These differences correspond to compressive strength differences of 4.65 MPa, 0.11 MPa, and 5.66 MPa (Fig. 5a). Comparing the model results with those of standard specimens, conversion factors of 2.48, 1.76, and 1.26 are obtained for the 50 mm, 75 mm, and 100 mm cores, respectively. A decrease in the ratios $f_{p(d)}/f_{c(150)}$ is observed regardless of the curing method of $f_{c(150)}$ compared to ordinary concrete with compressive strengths of about 25 MPa and 30 MPa [13].

The ratios $f_{p(d)}/f_{c(150)}$ also increase with the diameter (D) in the case of air curing (Fig. 5b). The experimental results for 100 mm cores require no corrections. These results are comparable to those obtained by Ju et al. [50] for

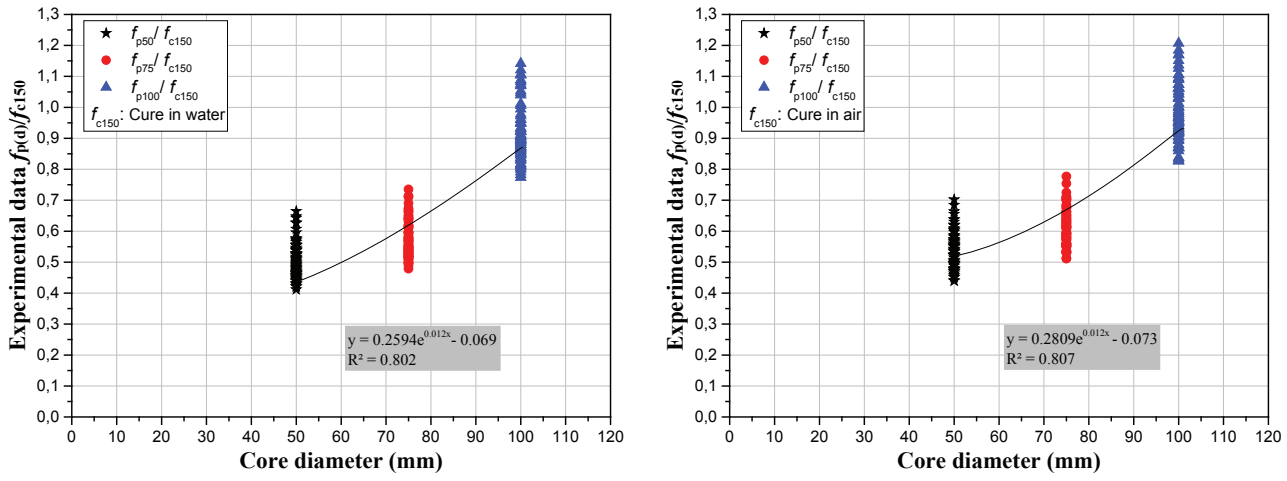

a) b)

Figure 5. Size effect for cores L/D=2. (a): Cure in water, (b): cure in air.

50 mm and 100 mm cores. However, the other two diameters necessitate conversion factors, although these remain lower when $f_{c(150)}$ is cured in water. Nevertheless, the fitting model encompassing all cores requires conversion factors of 2.3, 1.62, and 1.16 for the 50 mm, 75 mm, and 100 mm cores, respectively, compared to the standard specimen. However, the 100 mm cores conform to the conversion factors of ASTM C42 and EN 13791 [29, 30]. The compressive strength difference between the model and in-situ results for the 50 mm, 75 mm, and 100 mm cores is 5.56 MPa, 0.19 MPa, and 4.71 MPa, respectively. Overall, the compressive strength difference is acceptable, allowing us to assert that the proposed models align well with the experimental results.

The performance of the proposed models in terms of average prediction errors (RMSE) and standard deviations (SD) based on the number of cores is presented in Figure 6. This visualization provides insight into the predictive capability of the models as the number of cores increases. It is observed that increasing the number of cores decreases the prediction error, and consequently, the model is considered stable and reliable with at least 7 cores for the 100 mm and 50 mm cores (Fig. 6a). Several authors converge on the same conclusion, suggesting that the optimal number of cores is estimated between seven and nine [37, 38]. On the other hand, the 75 mm core stabilizes between 5 and 9 cores. In this curing case, the mean prediction error remains stable at 6.7 MPa, 2 MPa, and 5 MPa for the 100 mm, 75 mm, and 50 mm cores, respectively. The standard deviation (SD) of the model shows little variation beyond 6 cores for all three diameters (D) studied (Fig. 6b). As anticipated, there is a consistent pattern of stability in the average prediction errors (RMSE) and standard deviation (SD) during water curing. Conditional coring helps reduce uncertainties in the evaluation, along with the required number of cores, and consequently, the costs of in-situ tests.

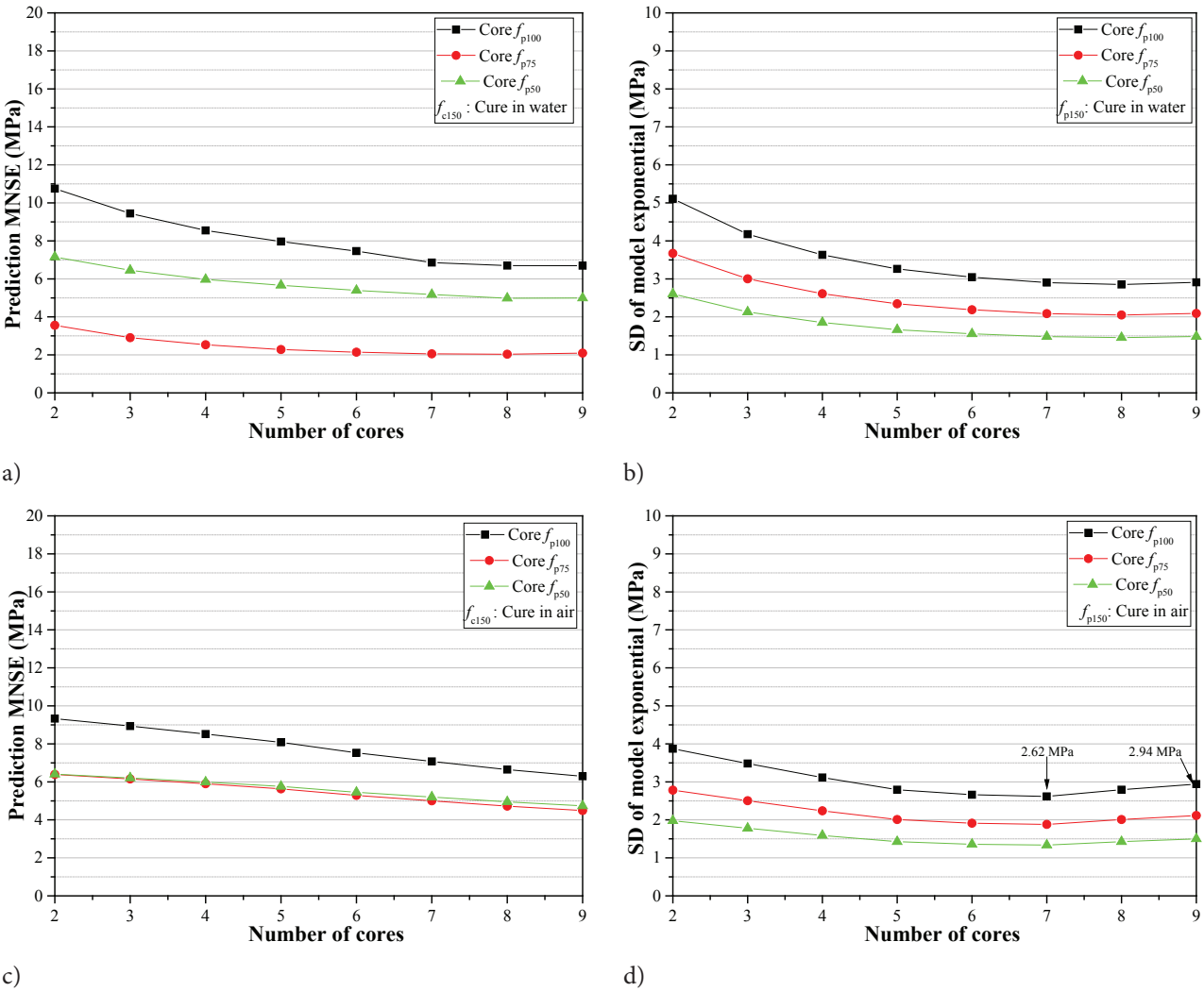

Figure 6. Influence of the number of cores on the error prediction RMSE and SD of the conversion model: Case of L/D=2. (a) and (b): Cure in water, (c) and (d): cure in air.

Table 8. Comparison of different cores with cast specimens (L/D=2)

	($f_{c(d)}$) cure in water		($f_{c(d)}$) cure in Air	
	f_{p100}/f_{c100}	f_{p50}/f_{c50}	f_{p100}/f_{c100}	f_{p50}/f_{c50}
Arithmetic mean	1.068	0.948	1.105	1.002
Standard Deviation	0.151	0.113	0.055	0.103
Coef of variation (%)	14.139	13.325	4.977	10.279

The curve in Figure 6c, related to air curing, indicates that the prediction error RMSE does not stabilize. Some authors suggest that nine cores are necessary to achieve stabilization [39, 40]. Following these combined or individual non-destructive testing (NDT) trials, Boussahoua et al. [66] observed that the minimum number of concrete strength evaluations is also nine. The comparison with $f_{c(150)}$ cured in the air has a negative effect, indicating that an increase in the number of cores becomes necessary. This may lead to structural instability and costly investments for destructive tests. The introduction of uncontrolled parameters confirms the disturbance of the model (Fig. 6d). Indeed, it is noticed that the standard deviation (SD) of the model increases slightly from 7 cores. However, it is important to note that this deviation remains relatively low, reaching only 0.32 MPa.

Table 8 compares the relationship between the compressive strength of cores and cast specimens of high-strength concrete with an L/D ratio of 2. A similar trend was observed; water curing decreases the ratios between cores and cast specimens. It is observed that these ratios are slightly higher or almost equal to 1. This facilitates the conversion of the compressive strength of cores. This observation can be explained by the cohesion of the concrete from cores extracted from blocks. It highlights the fact that the diameter of aggregates used in manufacturing does not influence compressive strength. However, these ratios show a significant decrease compared to ordinary concretes with strength below 40 MPa [13].

Case of Cast Specimens

Figure 7 illustrates the evolution of the compressive strength of cast specimens based on their diameter, distinguishing between those cured in water and air. An exponential improvement was observed in compressive strength with an increase in specimen diameter in both curing environments.

The exponential relationship of Equation 3 was also selected for the cast specimens. Compared with specimens $f_{c(150)}$ cured in water, it yielded a = 0.478, b = 0.0052, and c = -0.0351. On the other hand, specimens cured in air resulted in a = 0.429, b = 0.0061, and c = -0.0673. This correlation provides a better estimation of $\bar{f}_{c(d)}$. An improvement in the coefficient of determination (R^2) is observed, increasing from 0.544 for water curing to 0.663 for air curing. Similarly, the correlation coefficient (R) also experienced an improvement, rising from 0.737 in water curing to 0.814 in air curing.

The analysis of individual ratios for specimens cured in water, $f_{c(100)}/f_{c(150)}$, reveals that 24.69% of them have values greater than 1. The mean ratio for all specimens $f_{c(100)}/f_{c(150)}$ is 0.880. In contrast, $f_{c(50)}/f_{c(150)}$ ratios for specimens cured

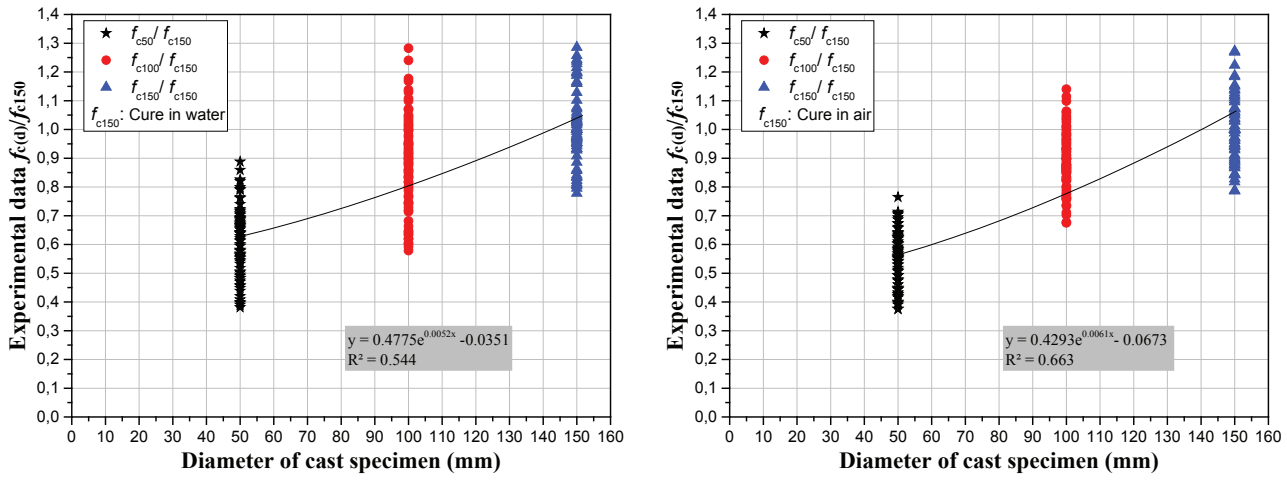

a) b)

Figure 7. Relationship between compressive strength of cast specimens and diameter (D). (a): Cure in water, (b): cure in air.

Table 9. Exponential equations as a function of (R) and (Vp)

References	Regression Formula (MPa)	Maximum strength (MPa)
Chen et al. [63]	$f_{cu} = 22.22e^{0.01926R} - 3.6$	< 70 MPa
Chen et al. [63]	$f_{cu} = 20.24e^{0.03049R} - 2.6$	≥ 70 MPa
Biswas et al. [64]	$f_{cu} = 27.87e^{0.000198Vp}$	79.40
Trtnik et al. [65]	$f_{cu} = 0.856e^{1.2882Vp}$	50
Atici [67]	$f_{cu} = 3.34e^{0.0598R}$	36.4
Atici [67]	$f_{cu} = 0.0316e^{1.3Vp}$	36.4
Mohammed et al. [68]	$f_{cu} = 9.5879\ e^{0.0384R}$	40

in water are all below 1, with an average value of 0.608. For specimens cured in open air, 19.75% of $f_{c(100)}/f_{c(150)}$ ratios are above 1, with an average value of 0.904. Additionally, $f_{c(50)}/f_{c(150)}$ ratios are all below 1, with an average of 0.533. These ratios decrease with specimen size. However, air curing improves the $f_{c(100)}/f_{c(150)}$ ratio while simultaneously decreasing the $f_{c(50)}/f_{c(150)}$ ratio. Compared to a recent study [13], it is observed that the use of high-strength concrete leads to a decrease in $f_{c(50)}/f_{c(150)}$ and $f_{c(100)}/f_{c(150)}$ ratios.

Comparisons with Other Studies

In this study, only exponential formulas were proposed to validate previously suggested equations. These formulas pertain to the compressive strength of concrete, estimated between 36.4 and 79.4 MPa.

Most research conducted in this field shows that exponential expressions provide a good prediction of compressive strength. The formulas presented in this study exhibit a relatively low RMSE. Consequently, the equations for estimating the compressive strength of high-strength concrete, by combining the most significant factors, can be useful on construction sites. Of course, further research is needed to refine the models proposed in this study.

CONCLUSION

In this study, a series of destructive tests (DT) was conducted on blocks cured in the open air, while another series was performed on cast high-strength concrete specimens cured in two different environments: open air and in water. The aim was to analyze the impact of specimen size, L/D ratio, and curing environment on compressive strength. The test results were compared to those of standard specimens to explore potential relationships for estimating average compressive strength. Various statistical indicators were employed to enhance this study. The obtained results lead to the following conclusions:

- The individual simulation of compressive strength for various ratios of $f_{p(d)}/f_{c(150)}$ led to the development of exponential equations, enabling an accurate estimation of the compressive strength of high-strength concrete. Indeed, the statistical indicators (CV) and (ARE) are lower in the case of exponential equations.
- Modeling the ratios $f_{p(d)}/f_{c(150)}$ as a function of the diameter (D) of the cores remains below 1. In this regard, the conversion models depend on the core size, the L/D ratio, and the curing environment. Indeed, reducing the size results in a significant decrease in the $f_{p(d)}/f_{c(150)}$ ratio, observed under constant L/D ratio and curing conditions.
- The transition from an L/D ratio of 1 to an L/D ratio of 2 in the case of wet curing results in a reduction of 3.24% for $f_{p(100)}/f_{c(150)}$, 6.34% for $f_{p(75)}/f_{c(150)}$, and 9.52% for $f_{p(50)}/f_{c(150)}$. There is a decrease of 4.55%, 7.13%, and 11.79% for cores of 50 mm, 75 mm, and 100 mm, respectively, in the case of air curing. The results highlight the significant impact of core size in the proposed models, underscoring its importance as a crucial parameter.
- Air curing leads to a decrease in the ratios $f_{p(d)}/f_{c(150)}$, especially when L/D=1. The core of 100 mm shows a reduction of 10.13%, while decreases of 8.64% and 10.33% are recorded for the 75 mm and 50 mm cores, respectively. However, core size has demonstrated a more significant influence compared to the two previously emphasized parameters.
- The effectiveness of our exponential models relies on various statistical indicators, including prediction errors (RMSE) and standard deviation (SD) of the conversion models. Comparison with water-cured standard cylindrical specimens allowed us to reduce the number of cores. Indeed, both statistical parameters stabilize, in wet curing, from 7 to 8, depending on the L/D ratio. However, when compared to air-cured standard cylindrical specimens, it was shown that at least 9 cores are needed. In practice, when the quality control level of the concrete is high, 7 cores may suffice.
- Given that this experimental study was conducted for a specific formulation and a w/c ratio of 0.43, additional experimental work involving other formulations, the direction of concrete flow, and L/D ratios equal to 1 for molded specimens would be necessary to further improve the precision and applicability of the developed models. This would contribute to the generalization of

prediction equations for high-strength concrete in engineering practice.
- Although the coring method of resistance evaluation is partially destructive, it remains the most reliable for evaluating compressive strength. The use of small-diameter cores is crucial for maintaining the structural stability of concrete structures.

AUTHORSHIP CONTRIBUTIONS

Authors equally contributed to this work.

DATA AVAILABILITY STATEMENT

The authors confirm that the data that supports the findings of this study are available within the article. Raw data that support the finding of this study are available from the corresponding author, upon reasonable request.

CONFLICT OF INTEREST

The author declared no potential conflicts of interest with respect to the research, authorship, and/or publication of this article.

ETHICS

There are no ethical issues with the publication of this manuscript.

REFERENCES

[1] Kang C, Park Y, Kim T. Evaluation of self-healing properties of OPC-slag cement immersed in seawater using UPV measurements. Materials 2023;16. [CrossRef]
[2] Oyunbileg D, Amgalan J, Batbaatar T, Temuujin J. Evaluation of thermal and freeze-thaw resistances of the concretes with the silica fume addition at different water-cement ratio. Case Stud Constr Mater 2023;19. [CrossRef]
[3] Kumar Mehta P, Monteiro PJM. Concrete microstructure, properties and materials. 3rd ed. Berkeley (CA): Department of Civil and Environmental Engineering, University of California at Berkeley; 2006.
[4] Gagan GS, Singh N. Reviewing the performance of concrete comprising recycled coarse aggregates using non-destructive tests. Mater Today Proc 2023;93:79–84. [CrossRef]
[5] Monteiro P, Miller S, Horvath A. Towards sustainable concrete. Nat Mater 2017;16:698–689. [CrossRef]
[6] Fares H. Mechanical and physico-chemical properties of self-placing concretes exposed to high temperature [dissertation]. Cergy-Pontoise (FR): University of Cergy-Pontoise; 2009.
[7] Yuva Y. Low-strength concrete properties in existing structures using NDT and core test results. J Build Eng 2023;76. [CrossRef]
[8] Jin L, Yu W, Du X, Zhang S, Li D. Meso-scale modeling of the size effect on dynamic compressive failure of concrete under different strain rates. Int J Impact Eng 2019;125:1–12. [CrossRef]
[9] Indelicato F. A statistical method for the assessment of concrete strength through microcores. Mater Struct 1993;26:261–267. [CrossRef]
[10] Seong-Tae Y, Eun-Ik Y, Joong-Cheol C. Effect of specimen sizes, specimen shapes, and placement directions on compressive strength of concrete. Nucl Eng Des 2006;236:116–127. [CrossRef]
[11] Gyengo T. Effect of type of test specimen and gradation of aggregate on compressive strength of concrete. J Proc 1938;34:269–283. [CrossRef]
[12] Murdock JW, Kesler CE. Effect of length to diameter ratio of specimen on the apparent compressive strength of concrete. ASTM Bull 1957;221:68–73.
[13] Merabti S. Effect of concrete class, maximum aggregate size and specimen size on the compressive strength of cores and cast specimens. Adv Mater Sci Eng 2022;22:21–31. [CrossRef]
[14] Neville AM. Properties of concrete. French ed. Paris: Edition Eyrolles; 2000.
[15] Fiore A, Porco F, Uva G, Mezzina M. On the dispersion of data collected by in situ diagnostic of the existing concrete. Constr Build Mater 2013;47:208–217. [CrossRef]
[16] Nsengiyumva W, Zhong S, Lin J, Zhang Q, Zhong J, Huang Y. Advances, limitations and prospects of nondestructive testing and evaluation of thick composites and sandwich structures: A state-of-the-art review. Compos Struct 2021;256. [CrossRef]
[17] Nedjar B. Damage mechanics: first gradient theory and application to concrete [dissertation]. Paris (FR): National School of Bridges and Roads; 1995.
[18] Alam SY, Loukili A, Grondin F. Monitoring size effect on crack opening in concrete by digital image correlation. Eur J Environ Civ Eng 2012;196:818–836. [CrossRef]
[19] Morel S. R-curve and size effect in quasibrittle fractures: Case of notched structures. Int J Solids Struct 2007;44:4272–4290. [CrossRef]
[20] Alam SY, Saliba J, Loukili A. Fracture examination in concrete through combined digital image correlation and acoustic emission techniques. Constr Build Mater 2014;69:232–242. [CrossRef]
[21] Hoover CG, Bažant ZP, Vorel J, Wendner R, Hubler MH. Comprehensive concrete fracture tests: description and results. Eng Fract Mech 2013;114:92–103. [CrossRef]
[22] Miano A, Ebrahimian H, Jalayer F, Prota A. Reliability estimation of the compressive concrete strength based on non-destructive tests. Sustainability 2023;15. [CrossRef]

[23] Naser AH, Badr AH, Henedy SN, Ostriwski KA, Imran H. Application of multivariate adaptive regression splines (MARS) approach in prediction of compressive strength of eco-friendly concrete. Case Stud Constr Mater 2022;17. [CrossRef]
[24] Chockalingam T, Vijayaprabha C, Leon Raj J. Experimental study on size of aggregates, size and shape of specimens on strength characteristics of pervious concrete. Constr Build Mater 2023;385. [CrossRef]
[25] Zhu R, Alam SY, Loukili A. An experimental investigation on the correlation between the aggregate size effect and the structural size effect. Eng Fract Mech 2020;234:107101. [CrossRef]
[26] Bocca P, Indelicato F. Size effects and statistical problems of microcores in the re-evaluation of existing structures. In: Proceedings of DABI Symposium; 1988 Sep; Copenhagen. p. 463–472.
[27] Sima J-II, Yang KH, Jeon JK. Influence of aggregate size on the compressive size effect according to different concrete types. Constr Build Mater 2013;44:716–725. [CrossRef]
[28] Kilinc K, Celik OA, Tuncan M, Tuncan A, Arslan G, Arioz O. Statistical distributions of in situ microcore concrete strength. Constr Build Mater 2012;26:393–403. [CrossRef]
[29] ASTM C42/C 42M-04. Standard method of obtaining and testing drilled cores and sawed beams of concrete. Philadelphia (PA): American Society for Testing and Materials; 2001.
[30] EN 13791:2019. Assessment of in-situ compressive strength in structures and precast concrete components. Brussels (BE): European Committee for Standardization; 2019. p. 41.
[31] ISO/DIS 7032. Cores of hardened concrete - Taking examination and testing in compression. Geneva (CH): International Organization for Standardization; 1983.
[32] DIN 1048 Teil 2. Prüfverfahren für Beton. Bestimmung der Bruchfestigkeit von Festbeton in Bauwerken und Bauteilen. Berlin (DE): Deutsches Institut für Normung; 1991.
[33] ACI 301-84. Specification for structural concrete for buildings. Detroit (MI): American Concrete Institute; 1984.
[34] Bungey JH. Determining concrete strength by using small diameter cores. Mag Concr Res 1979;31:91–98. [CrossRef]
[35] Emilia V, Donato C, Angela C, Luprano IAM. Estimating in situ concrete strength combining direct and indirect measures via cross-validation procedure. Constr Build Mater 2017;151. [CrossRef]
[36] Alwash M, Breysse D, Sbartaï ZM. Nondestructive strength evaluation of concrete: analysis of some key factors using synthetic simulations. Constr Build Mater 2015;99:235–245. [CrossRef]
[37] Boussahoua Y, Kenai S, Ali-Benyahia K. Prediction of concrete strength by non-destructive testing in old structures: Effect of core number on the reliability of prediction. MATEC Web Conf 2018;149. [CrossRef]
[38] Alwash M, Sbartaï ZM, Breysse D. Non-destructive assessment of both mean strength and variability of concrete: A new bi-objective approach. Constr Build Mater 2016;113:880–889. [CrossRef]
[39] Ali-Benyahia K, Sbartaï ZM, Breysse D, Ghrici M, Kenai S. Improvement of nondestructive assessment of on-site concrete strength: Influence of the selection process of cores location on the assessment quality for single and combined NDT techniques. Constr Build Mater 2019;195:613–622. [CrossRef]
[40] Ali-Benyahia K, Sbartaï ZM, Breysse D, Kenai S, Ghrici M. Analysis of the single and combined non-destructive test approaches for on-site concrete strength assessment: General statements based on a real case-study. Case Stud Constr Mater 2017;6:109–119. [CrossRef]
[41] ACI 228.1R-19. Report on methods for estimating in-place concrete strength. Farmington Hills (MI): American Concrete Institute; 2019.
[42] NA 17004. Evaluation de la résistance à la compression sur site des structures et les éléments préfabriqués en béton. Alger (DZ): IANOR; 2008.
[43] Indelicato F. Estimation of concrete cube strength by means of different diameter cores: A statistical approach. Mater Struct 1997;24:131–138. [CrossRef]
[44] ACI CODE-318-19(22). Building code requirements for structural concrete and commentary. Farmington Hills (MI): American Concrete Institute; 2022.
[45] ACI 214.4R-10. Guide for obtaining cores and interpreting compressive strength results. Farmington Hills (MI): American Concrete Institute; 2016.
[46] EN 1998-1:2005/A101:2009/AC. Design of structures for earthquake resistance - Part 1: General rules, seismic actions and rules for buildings. Brussels (BE): CEN; 2022.
[47] Merabti S, Bezari S. Study of stress distribution in L-shaped walls with openings under intense seismic conditions on various soil types. J Eng Exact Sci 2023;9. [CrossRef]
[48] Merabti S, Bezari S, Laari AA, Khachouche A. Investigation into the impact of L-shaped RC shear wall placement with openings on the behavior of medium-rise buildings. J Eng Exact Sci 2023;9. [CrossRef]
[49] Merabti S, Guelmine L. Influence of concrete compressive strength on L-shaped shear wall performance in buildings within high-seismicity zones. J Eng Exact Sci 2024;10. [CrossRef]
[50] Ju M, Park K, Oh H. Estimation of compressive strength of high strength concrete using non-destructive technique and concrete core strength. Appl Sci 2017;7:1–16. [CrossRef]

[51] Wankhade RL, Landage AB. Non-destructive testing of concrete structures in Karad region. Procedia Eng 2013;51:8–18. [CrossRef]
[52] Jain A, Kathuria A, Kumar A, Verma V, Murari K. Combined use of nondestructive tests for assessment of strength of concrete in structure. Procedia Eng 2013;54:241–251. [CrossRef]
[53] Ivanchev I. Assessment of in-situ concrete compressive strength in RC structures by destructive and non-destructive methods. AIP Conf Proc 2023;2887. [CrossRef]
[54] Shrestha B, Giri OP. Study on concrete compressive strength through destructive and non-destructive testing. Int J Sci Math Technol Learn 2023;31.
[55] ACI Committee 213R-14. Guide for structural lightweight-aggregate concrete. Farmington Hills (MI): American Concrete Institute; 2014.
[56] DTR BC, 2 48. Algerian seismic code - RPA 99 version 2003. Algiers (DZ): National Centre for Applied Research in Paraseismic Engineering (CGS); 2003.
[57] ASTM C469. Standard test method for static modulus of elasticity and Poisson's ratio of concrete in compression. In: Annual Book of ASTM Standards. Philadelphia (PA): ASTM; 2010. p. 255-8.
[58] ASTM C39. Standard test method for compressive strength of cylindrical concrete specimens. In: Annual Book of ASTM Standards. Philadelphia (PA): ASTM; 2001.
[59] NA 5071. Tests for concrete in structures: cores sampling, examination and testing compression. Algiers (DZ): Algerian Institute of Standardization; 2005.
[60] EN 12504-1. Testing concrete in structures - Part 1: Cored specimens - Taking, examining and testing in compression. Berlin (DE): Beuth Verlag; 2016.
[61] Breysse D. Nondestructive evaluation of concrete strength: An historical review and a new perspective by combining NDT methods. Constr Build Mater 2012;33:139–163. [CrossRef]
[62] Amini K, Jalalpour M, Delatte N. Advancing concrete strength prediction using non-destructive testing: Development and verification of a generalizable model. Constr Build Mater 2016;102:762–768. [CrossRef]
[63] Chen J, Jin DQ, Dong C. Research on the rebound hammer testing of high-strength concrete's compressive strength in the Xinjiang region. Buildings 2023;13. [CrossRef]
[64] Biswas R, Rai B, Samui P. Compressive strength prediction model of high strength concrete with silica fume by destructive and non-destructive technique. Infrastruct Solut 2021;6:65. [CrossRef]
[65] Trtnik G, Kavčič F, Turk G. Prediction of concrete strength using ultrasonic pulse velocity and artificial neural networks. Ultrasonics 2009;49:53–60. [CrossRef]
[66] Boussahoua Y, Kenai S, Sbartaï ZM, Breysse D, Ali-Benyahia K. Influence of the number of cores on concrete strength assessment by nondestructive tests in old existing structures. Asian J Civ Eng 2023;24:1–15. [CrossRef]
[67] Atici U. Prediction of the strength of mineral admixture concrete using multivariable regression analysis and an artificial neural network. Expert Syst Appl 2011;38:9609–9618. [CrossRef]
[68] Mohammed BS, Azmi NJ, Abdullahi M. Evaluation of rubbercrete based on ultrasonic pulse velocity and rebound hammer tests. Constr Build Mater 2011;25:1388–1397. [CrossRef]